

A RF-MEMS switchable CPW air-bridge

Adrián Contreras^{*}, Jasmina Casals-Terré[#], Lluís Pradell^{*}

^{*}Signal Theory and Communications Department

[#]Mechanical Engineering Department

Technical University of Catalonia (UPC)

Barcelona, Spain

Flavio Giacomozzi, Sabrina Colpo, Jacopo Iannacci

MEMS group

Fondazione Bruno Kessler (FBK)

Trento, Italy

Miquel Ribó

Engineering Department

La Salle – Ramon Llull University

Barcelona, Spain

Abstract— This work presents a new shunt-type ohmic contact RF-MEMS switch specifically designed as a switchable CPW air bridge. The switch can be used in coplanar waveguide (CPW) reconfigurable multimodal circuits, for a selective use of the CPW odd-mode. The bridge is anchored using folded-beam suspensions, in such a way that two points at each end of the bridge remain free to contact the ground planes of the CPW. The suspension has been designed to compensate stress gradients effects and to lower actuation voltage. In the actuated (ON) state, the switch isolation to the odd mode is better than 20dB up to 8GHz and 10dB up to 30GHz.

Keywords—RF MEMS switch; coplanar waveguide; multimodal circuit.

I. INTRODUCTION

A significant effort has been devoted to the development of high-performance microwave circuits using RF MEMS [1]. In most cases these circuits are uniplanar, because they use coplanar waveguides (CPW) or, in a few cases, slotlines [2]. Since the CPW is able to propagate two fundamental modes (the even mode and the odd mode), it can be considered as a multimodal transmission line. While the even mode is widely used in common CPW circuits, the odd mode is considered as spurious and short-circuited by means of air bridges wherever it is generated (at transitions and asymmetries). However, it provides an additional degree of freedom in CPW designs. Recently, new kinds of CPW circuits based on the multimodal concept have been proposed [3-6]. In contrast with conventional CPW circuits, multimodal CPW ones allow the combined and controlled propagation of even and odd modes in some CPW sections. One key advantage of these circuits is the possibility of independent control of one of the modes, leaving the other unaffected. This feature was used in [4], [5] to design reconfigurable multimodal phase switches that use either ohmic- or capacitive-contact MEMS switches for the selective control of the CPW-even mode. In [6], PIN diodes were used to control the odd mode in a multimodal bandpass filter with reconfigurable fractional bandwidth. However, to

the authors' knowledge, a selective control of the CPW-odd mode using RF-MEMS switches has not yet been reported in the literature.

In this paper, a RF-MEMS reconfigurable air-bridge that behaves as a switchable short-circuit for the odd mode is proposed. A combination of folded-beam suspensions and a reinforced membrane gives place to a robust structure against either positive or negative stress gradients. In addition, the pull-in voltage is reduced thanks to the folded-beam suspension [7]. The proposed switch can also be used in a wide variety of slotline MEMS tunable circuits. This paper is organized as follows: section II presents the mechanical aspects and main fabrication details of the device; section III presents RF performance and the equivalent odd-mode circuit of the switch; finally, section IV summarizes the conclusions drawn from this work.

II. FABRICATION PROCESS AND MECHANICAL DESIGN

The technology used for the fabrication of the switch consists of an eight-mask surface micromachining process from FBK [8]. Fig. 1 shows a cross section which describes the structural capabilities of the process. In this technology, two gold layers of different thicknesses can be electrodeposited to define transmission lines and suspended membranes. The movable bridges are manufactured using a 1.8- μm -thick gold layer and a second 3.5- μm -thick superimposed gold film to increase the rigidity of selected parts of the membranes. For the proposed switch, two different thicknesses of photoresist sacrificial layer have been used, 3 μm and 1.6 μm in order to obtain a final air gap of 2.7 μm and 1.3 μm respectively. The DC actuation pads, bias lines and contact bumps are defined by using high resistivity polysilicon. A Ti-TiN-Al multilayer is used as "underpass" to connect signal lines under suspended structures. A third 150-nm gold layer is evaporated over the underpass metal line for manufacturing the low-resistance metal-to-metal electromechanical contacts.

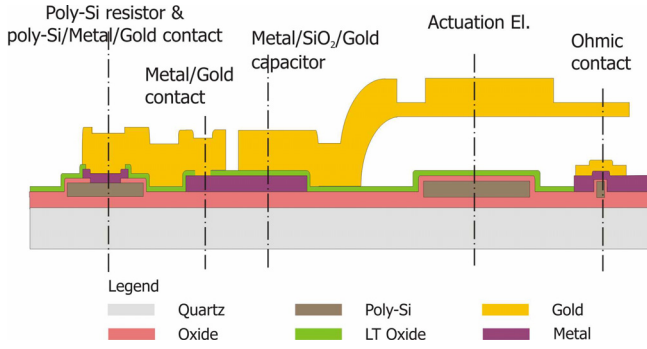


Fig. 1. Cross-section view of the FBK-first RF-MEMS fabrication process for ohmic-contact switches.

The fabricated switch is shown in Fig. 2. The structure is composed by a reinforced gold membrane with two ohmic contacts, on top and bottom edges, respectively. The bridge has a window in the center part to reduce the capacitance seen by the even mode of the CPW. The membrane is anchored to isolated islands by folded beam suspensions, made of a 1.8- μm thick, 10- μm wide single gold layer. The folded beam suspension was chosen due to its capability to compensate for intrinsic residual stresses induced by the fabrication process and provide low spring constant values in a compact area.

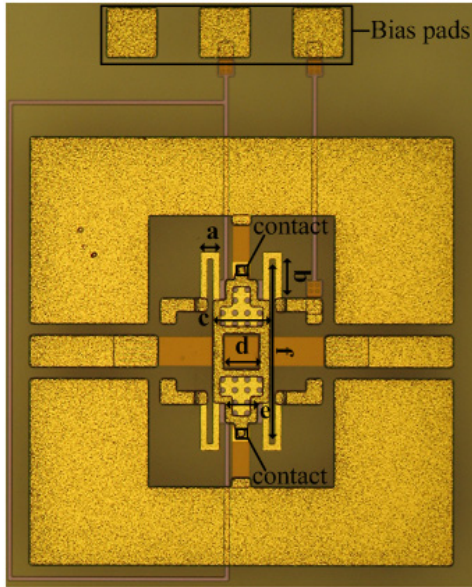


Fig. 2. Fabricated shunt ohmic switch.

The spring constant (without stress effects) can be estimated using [9]

$$k \approx \frac{24EI}{L_b^3}, \quad (1)$$

where E is the Young's modulus, L_b is the length of the supporting beams and $I = w_b t_b^3 / 12$ is the moment of inertia, with t_b , w_b being the beam thickness and beam width, respectively. When the actuation voltage (higher than the pull in voltage V_{pi}) is applied to the electrodes, the bridge contacts

touch the 150-nm gold layer over the underpass line, which is connected to the ground planes of the CPW. The static pull-in voltage is given by:

$$V_{pi} = \sqrt{\frac{8kg_0^3}{27A\epsilon_0}}. \quad (2)$$

In (2), g_0 is the initial gap between the membrane and the polysilicon electrode, A is the area of the actuation pads and ϵ_0 is the permittivity of air. The area of each polysilicon electrode is 90 $\mu\text{m} \times 85 \mu\text{m}$. The calculated spring constant using (1) is $k = 12.9 \text{ N/m}$. According to finite element simulations (ANSYSTM) the stiffness constant is $k = 13.3 \text{ N/m}$. Thus, for the devices with $g_0 = 2.7 \mu\text{m}$, the expected pull-in voltage (2) is $V_{pi} = 24 \text{ V}$. However, the measured voltage is $V_{pi} = 26 \text{ V}$. For switches with $g_0 = 1.3 \mu\text{m}$, the measured pull-in voltage is $V_{pi} = 12 \text{ V}$, which is 4V higher than the calculated one using (2). This could be attributed to small differences in both the thickness of gold layers and the gap between electrodes (g_0). The dimensions and mechanical parameters of the proposed switch are shown in table I.

TABLE I
DIMENSIONS AND PARAMETERS FOR THE ODD-MODE SWITCH

Parameter	$g_0: 1.3 / 2.7 \mu\text{m}$
Meander length, a (μm)	30
Supporting beams width, (μm)	10
Supporting beams length, b (μm)	78
Bridge width 1, c (μm)	90
Window width, d (μm)	60
Bridge width 2, e (μm)	50 μm
Bridge length, f (μm)	275
Ohmic contact area, (μm^2)	10 \times 12
Spring constant*, k (N/m)	13.3
Pull-in voltage, V_{pi} (V)	12 / 26
Pull-out voltage, V_{po} (V)	8 / 21

The mechanical design of the switch is aimed to be more robust against stress gradients, which could create problems for typical CPW ground-plane separations. Besides the use of folded beam suspensions, a 3.5- μm frame minimizes the bending of the central part of the bridge.

The height of ohmic contacts placed on the top and bottom electrodes could be affected by stress gradients during fabrication. The deformation of the bridge due to stress gradients has been simulated using ANSYSTM. The structure can handle positive and negative stress gradients without compromising the function of the switch. Fig. 3 shows the deformation of the bi-layer membrane, where the initial stress values used for the simulation are $\sigma_2 = 58 \text{ MPa}$ (gold layer with a thickness $t_2 = 1.8 \mu\text{m}$) and $\sigma_1 = 62 \text{ MPa}$ (gold layer with a thickness $t_1 = 3.5 \mu\text{m}$). For this case, the simulated maximum deflection is less than 0.07 μm .

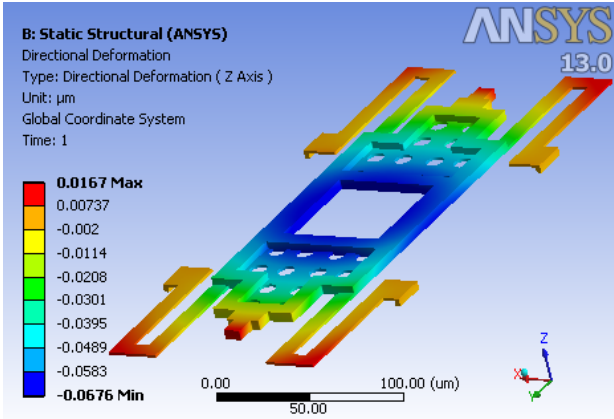


Fig. 3. Simulated deformation due to stress gradient effects.

Fig. 4 shows optical-profiler results of the fabricated device. As can be seen, the main membrane is almost flat. There is a very small negative stress gradient; this has little effect in the stiffness constant of the device.

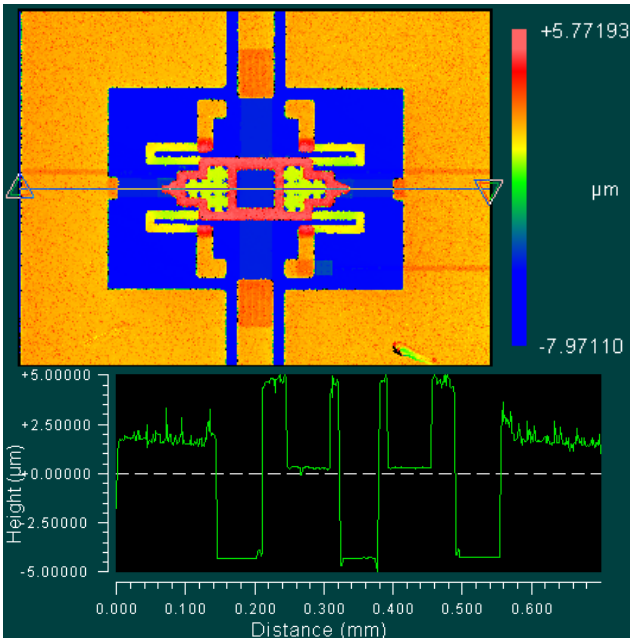


Fig. 4. Optical profiler results of the fabricated switch.

III. RF MEASUREMENTS

The switch of Fig. 2 was implemented on a CPW test-circuit composed of CPW sections with different dimensions due to fabrication and measurement constraints. The outer CPW sections feature 20- μm slots and a 50- μm central strip, resulting in characteristic even- and odd-mode impedances $Z_{0e1} = 75 \Omega$ and $Z_{0o1} = 100 \Omega$, respectively. The inner CPW section features 195- μm slots instead, resulting in characteristic even- and odd-mode impedances $Z_{0e2} = 145 \Omega$ and $Z_{0o2} = 195 \Omega$, respectively.

The measured hysteresis of the shunt ohmic switch with a 1.3- μm air gap is shown in Fig. 5. The pull-in voltage was measured when the isolation is higher than 20 dB at 50 MHz.

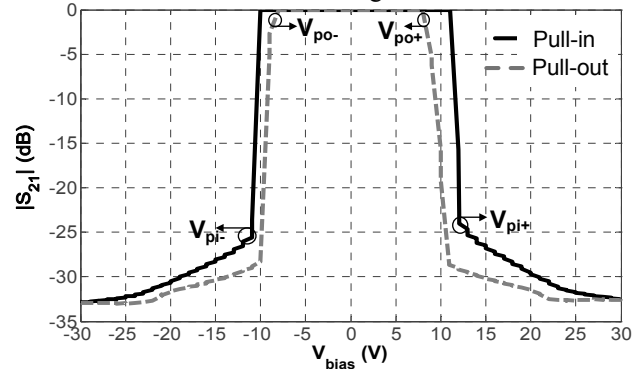


Fig. 5. Measured hysteresis (at $f = 50$ MHz) of an ohmic switch with $g_0 = 1.3 \mu\text{m}$.

The RF performance of four different ohmic switches, with respect to the odd mode was measured using 150 μm -pitch SG-GS probes, as shown in Fig. 6. The S parameters of the high impedance CPW line where the switch is actually placed were obtained from de-embedding of the low-impedance input and output sections. After normalizing with the proper characteristic impedance, it can be seen that the insertion loss of the switch in the “up” state is smaller than 1.2 dB and the isolation in the “down” state is better than 20 dB up to 8 GHz and 10 dB up to 30 GHz, as shown in Fig. 7.

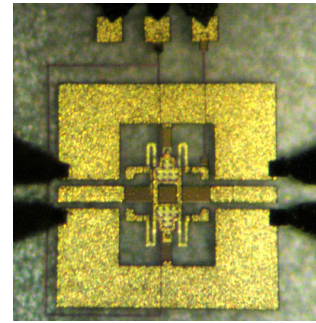


Fig. 6. Measurement of the switch using SG-GS probes.

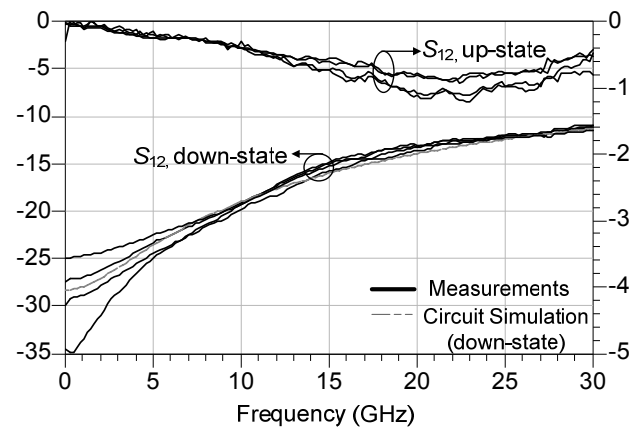


Fig. 7. Measured CPW odd-mode insertion loss (up state) and isolation (down state) of four different ohmic switches (1.3- μm and 2.7- μm air gap).

Using measured data, the circuit model of Fig. 8 was obtained. The total inductance of the switch is $L_t = 0.18$ nH and its total resistance is $R_t = 2$ Ω . This includes the effect of the underpass line and the ohmic-contact resistances. The applied voltage during measurements was $1.4V_{pi} = 36.4$ V.

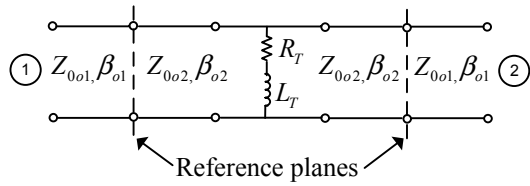


Fig. 8. Equivalent circuit model (for CPW-odd mode) when the switch is in the down state, $R_T = 2$ Ω and $L_T = 0.18$ nH. β_{o1}, β_{o2} are the odd-mode phase constants.

The influence of the switch on the even mode is mainly capacitive. After measuring the switch using GSG probes, it was found that the capacitance in the down state is $C_{pe} = 0.095$ pF. The effect of C_{pe} over the even -mode S parameters is shown in Fig. 9.

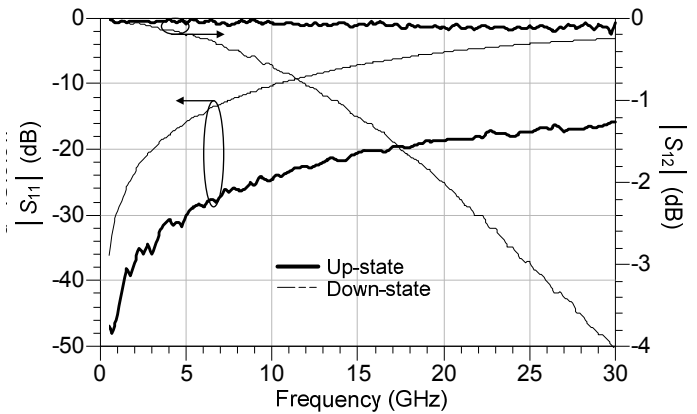


Fig. 9. Even-mode measured S -parameters for both states.

IV. CONCLUSION

In this work, a bridge-type double-contact ohmic switch for switchable/reconfigurable air bridges has been presented. The switch can be used in CPW multimodal circuits to short circuit the odd-mode, or in slotline circuits. The performance of the device has been measured for both fundamental modes of the CPW. The measured odd-mode isolation is higher than 20 dB up to 8 GHz and 10 dB up to 30 GHz. Although the even-mode capacitance C_{pe} of the switch is small, it has a considerable effect over the performance of the switch.

The CPW even mode performance can be improved by using wider underpass lines (in this case, these are connected to the CPW ground planes). C_{pe} could be reduced by using narrow center beams (less than 15- μ m, if design rules allow it).

ACKNOWLEDGMENT

This work has been supported by project TEC2010-20318-C02 and the fellowship BES-2008-004923 from the Spanish

Ministry of Science and Innovation. The authors would like to thank the staff of FBK MT-Lab for the support in the fabrication of the RF-MEMS devices.

REFERENCES

- [1] S. Lucyszyn, "Review of radio frequency microelectromechanical systems technology," *Science, Measurement and Technology, IEE Proceedings*, vol.151, no.2, pp. 93–103, March 2004.
- [2] K. Van Caekenberghe, T. Vaha-Heikkila, "An Analog RF MEMS Slotline True-Time-Delay Phase Shifter," *IEEE Transactions on Microwave Theory and Techniques*, vol.56, no.9, pp.2151–2159, September 2008.
- [3] M.A. Llamas, M. Ribó, D. Girbau, L. Pradell, "A Rigorous Multimodal Analysis and Design Procedure of a Uniplanar 180° Hybrid," *IEEE Transactions on Microwave Theory and Techniques*, vol. 57, no. 7, pp. 1832 – 1839, July 2009.
- [4] M. A. Llamas, D. Girbau, M. Ribó, L. Pradell, A. Lázaro, F. Giacomozzi, and B. Margesin, "MEMS-based 180° phase switch for differential radiometers," *IEEE Transactions on Microwave Theory and Techniques*, vol.58, no.5, pp. 1264–1272, May 2010.
- [5] M. A. Llamas, D. Girbau, M. Ribó, L. Pradell, F. Giacomozzi, and S. Colpo, "RF-MEMS Uniplanar 180 Phase Switch Based on a Multimodal Air-Bridged CPW Cross", *IEEE Transactions on Microwave Theory and Techniques*, vol.59, no.7, pp. 1769–1777, July 2011.
- [6] A. Contreras, L. Pradell, M. Ribó "A Novel Tunable Multimodal Bandpass Filter" *41st European Microwave Conference EuMC-2011 Proceedings*, pp. 1059-1062, Manchester, UK, 9–14 Oct. 2011
- [7] D. Peroulis, S. P. Pacheco, K. Sarabandi, and L. P. B. Katehi, "Electromechanical considerations in developing low-voltage RF MEMS switches", *IEEE Transactions on microwave theory and techniques*, vol. 51, no. 1, pp. 259–270, January 2003.
- [8] F. Giacomozzi, V. Mulloni, S. Colpo, J. Iannacci, B. Margesin, A. Faes, "A flexible technology platform for the fabrication of RF-MEMS devices", *2011 International Semiconductor Conference (CAS)*, vol.1, pp.155-158, Sinaia, Romania, 17–19 October 2011.
- [9] G. M. Rebeiz, *RF MEMS, Theory, Design and Technology*, New York, J. Wiley & Sons, 2003.